2020 SAE AERO DESIGN WEST COMPETITION

FORT WORTH, TEXAS

APRIL 3-5, 2020

Union College Flying Dutchmen Advanced Design Report

Union College, Team 215

Co-Authors

Alexander BRUNO

Roderick LANDRETH

Kevin CARO

Joana SANTOS

Mustafa KHAN

Faculty Advisors

Dr. Bradford BRUNO

Dr. John SPINELLI

Dr. Shawn WEHE

STATEMENT OF COMPLIANCE

Certification of Qualification

Team Name	Union College Flying Dutchmen Advanad	Team Number	215
School	Union College, NY		
Faculty Advisor	Bradford Bruno		
Faculty Advisor's Email	brunob@union.edu		

Statement of Compliance

As faculty Adviser:

BB (Initial) I certify that the registered team members are enrolled in collegiate courses.

BB (Initial) I certify that this team has designed and constructed the radio-controlled aircraft in the past nine (9) months with the intention to use this aircraft in the **2020** SAE Aero Design competition, without direct assistance from professional engineers, R/C model experts, and/or related professionals.

BB (Initial) I certify that this year's Design Report has original content written by members of this year's team.

BB (Initial) I certify that all reused content have been properly referenced and is in compliance with the University's plagiarism and reuse policies.

BB (Initial) I certify that the team has used the Aero Design inspection checklist to inspect their aircraft before arrival at Technical Inspection and that the team will present this completed checklist, signed by the Faculty Advisor or Team Captain, to the inspectors before Technical Inspection begins.

Bradford Bruno — Signature of Faculty Advisor — 2/19/20 — Date

[signature] — Signature of Team Captain — 2/19/20 — Date

Contents

List of Figures

List of Tables

1 Executive Summary

1.1 Team Management

Union College is a small liberal arts school with an ABET accredited engineering program. At Union, engineering students take classes in the arts and humanities on top of their major requirements, creating a well-rounded college experience. The SAE Aero Club at Union College is made up of first, second and third year students which compete in the SAE Aero Micro Class Competition. The advanced class comprises five engineering students from the mechanical and electrical engineering departments and participate in the SAE Aero Advanced Class Competition to fulfill part of their senior project requirement. Together, the micro and advanced classes make up the Union College Aero Team. To stay organized, the team fabricated Gantt charts, used online drives to store and share files, and met weekly to discuss progress and plan for future work. The Gantt Chart is summarized under Design Schedule.

1.2 System Overview

Our aircraft's rectangular high wing is located above the fuselage and incorporates plain flaps as HLDs. Low lift gliders are mounted under the wing and close to the fuselage using standoffs. Under the wing, a fuselage shell connected to a fairing leads from the cargo bay to the tail. Our design also includes a conventional tail, tricycle type landing gear, and a nose cone. Our entire aircraft costs approximately $2530.

1.3 Competition Projections and Innovations

Our goal is to transport 18 habitat modules, 8 water bottles, and two Colonist Delivery Aircraft (CDA), each containing 30 colonists, weighing a total of 10 lbs. For five rounds at competition, our score goal is 59.4 points. Design innovations integrated into our design include using expanded polystyrene (EPS) foam to manufacture the wings allowing for weight reduction and rapid manufacturability, the design of a new model for the CDA using a 3D printed, carbon fiber frame, a newly designed hinge which connects the control surfaces to the lifting surfaces, and the use of a quad-copter motor. With these innovations, we intend to gain an advantage over other teams and make our design more reliable.

2 Design Schedule

The schedule breaks down into three major phases:

Phase 1: Research and design (September - December)

- Analysis of the scoring equation
- Definition and optimization of the design space
- Preliminary design decisions and modeling (number of motors, location of wing, etc.)
- CDA design and modeling (delta wing, flying wing, conventional airframe etc.)

Phase 2: Refine design and build (December - February)

- Finalize mothership and CDA design
- Perform dynamic stability calculations for airframe layout
- Perform thrust and minimum propeller airspeed calculations
- Build the mothership and CDAs
- Program autopilot on pre-built test bed

Phase 3: Test (February - April)

- Perform dynamic tests (taxi aircraft, find minimum take off length and max bank angle)
- Test CDA with autopilot
- Gather required data from dynamic tests
- Test limits of operating envelope for aircraft

3 Design and Justification

3.1 Overall Design Description

Our design was divided into five subassemblies that include the nose cone, fuselage, wings, fairing and tail sections, all held together through a carbon fiber boom that runs along the longitudinal axis of the aircraft. The nose cone, fuselage and fairing feature a continuous streamline body designed to minimize drag and enclose all electronics and payload. The nose cone and fuselage are constructed using a set of ribs wrapped with a layup of balsa wood, carbon fiber and epoxy. The fairing is also made of ribs, connected using a set of longerons and wrapped with UltraCote, a thin, lightweight film of plastic.

We are using a single, rectangular, cantilever high wing, located above the fuselage. Our tail is conventional and located aft of the fuselage. The plane is supported by fixed, tricycle type landing gear. Ailerons, elevators and a rudder make up the primary control surfaces and a pair of flaps make up the secondary control surfaces.

Our aircraft uses a T-Motor U8 Lite 190 KV, with a 28.4 x 10.1 inch propeller. These parts provide sufficient thrust for our model which was designed to takeoff with a maximum weight of 25 lbs, a wingspan of 124 inches, and a tip to tail length of 110 inches. Figure 1 shows a drawing of our plane modeled on SOLIDWORKS. Trade studies used to select the aircraft configuration are shown in the Design Details section.

A full cost break down is described in Table 1.

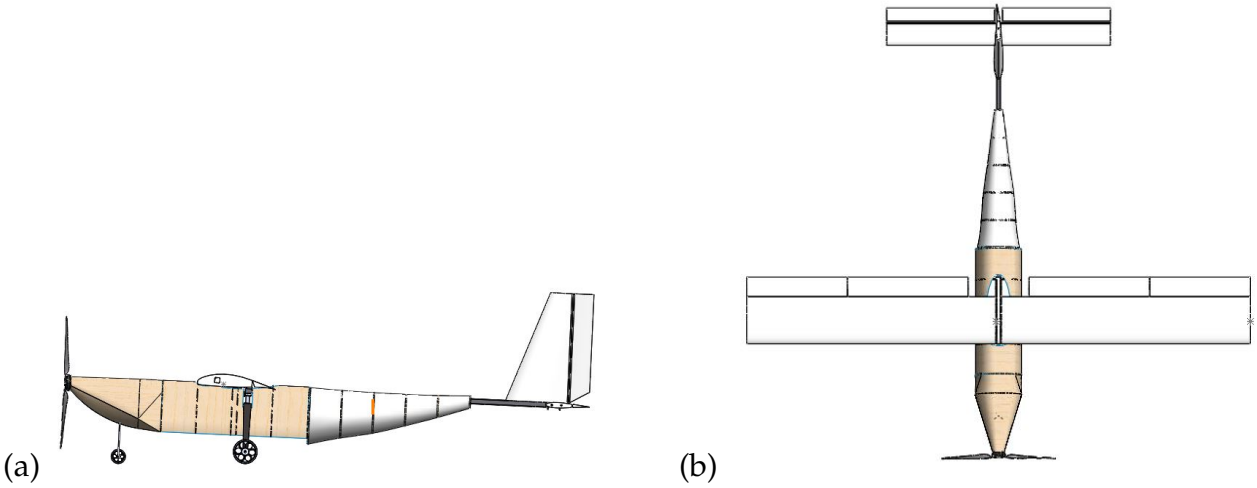

(a) (b)

Figure 1: Full Plane Model Side View (a) and Top View (b).

Table 1: Aircraft Cost Breakdown

Components	**Cost**	**Items**
Wing	$350	Foam, Hinges, UltraCote, Spar
Fuselage	$540	Balsa wood, Carbon Fiber sheets, Spar, UltraCote, Landing Gear, Wheels
Tail	$100	Foam, UltraCote, Carbon Fiber shafts, Hinges
Electronics	$1440	Motor, Battery, Controllers, Ground station, Cameras, GPS, Servos
Miscellaneous	$100	Epoxy, Fasteners, PLA
Total	$2530	

3.2 Scoring and Sensitivities

3.2.1 Scoring Analysis and Optimization

Before optimizing the scoring algorithm, the design space had to be well defined. This was done based on maximum payload capacity estimates from past teams's planes. This experience led us to pick a maximum payload capacity of 15 pounds. After that was established, the design space for the colonist gliders had to be established. This was done by forming a rough estimate of the weight of the airframe and electronics based on a theoretical sensor suite and fuselage design. The remaining weight allowance, after subtracting the weight of the airframe and electronics, was then used to calculate the maximum number of colonists that could be carried (30 in this case) based on the average weight of each colonist (ping pong balls) this then fully defined the design space on which we wanted to optimize for maximum score. This was done by doing an exhaustive search on the entire design space, and finding the configuration would yield the highest score. This was not complete, since it is impossible to have a 100% accuracy rate for payload drops. Therefore a conservative drop accuracy of 25% was assumed based on past team performance, as well as advice from subject matter experts. Based on the defined design space and chosen accuracy, the maximum potential flight score was calculated to be 59.4. The breakdown of payload carried, and delivered based on 25% drop accuracy and 50% colonist accuracy can be seen in the table below.

Table 2: Payload Projection Layout

Payload Delivered (25% Accuracy)		Payload needed to be carried	
Colonists Delivered (Nc)	242	Colonists Carried Per glider	30
Habitats Delivered (Nh)	21	Habitats carried per round	18
Amount of Water Delivered (fl oz)	168	Amount of Water carried per round	304
Static Payload	0	Static Payload	0

As seen in the table above, zero pounds of static payload is suggested, as droppable payload yields many more points per ounce than static payload does, but static payload delivers points regardless of drop accuracy. The design space was also plotted, ignoring the static payload as

all optimized, or nearly optimized states have zero static payload. The function was plotted in three dimensions and color to represent the four important variables: number of habitats, amount of water, number of colonists, and score (Score is the Z axis, and number of Colonists delivered is represented by the color gradient). This was not plotted in four dimensions as 4-D screens have not yet been developed to our knowledge. The 3D-plus-color point cloud can be seen below. This was done to visualize the sensitivity of the scoring function to changes in the payload delivered.

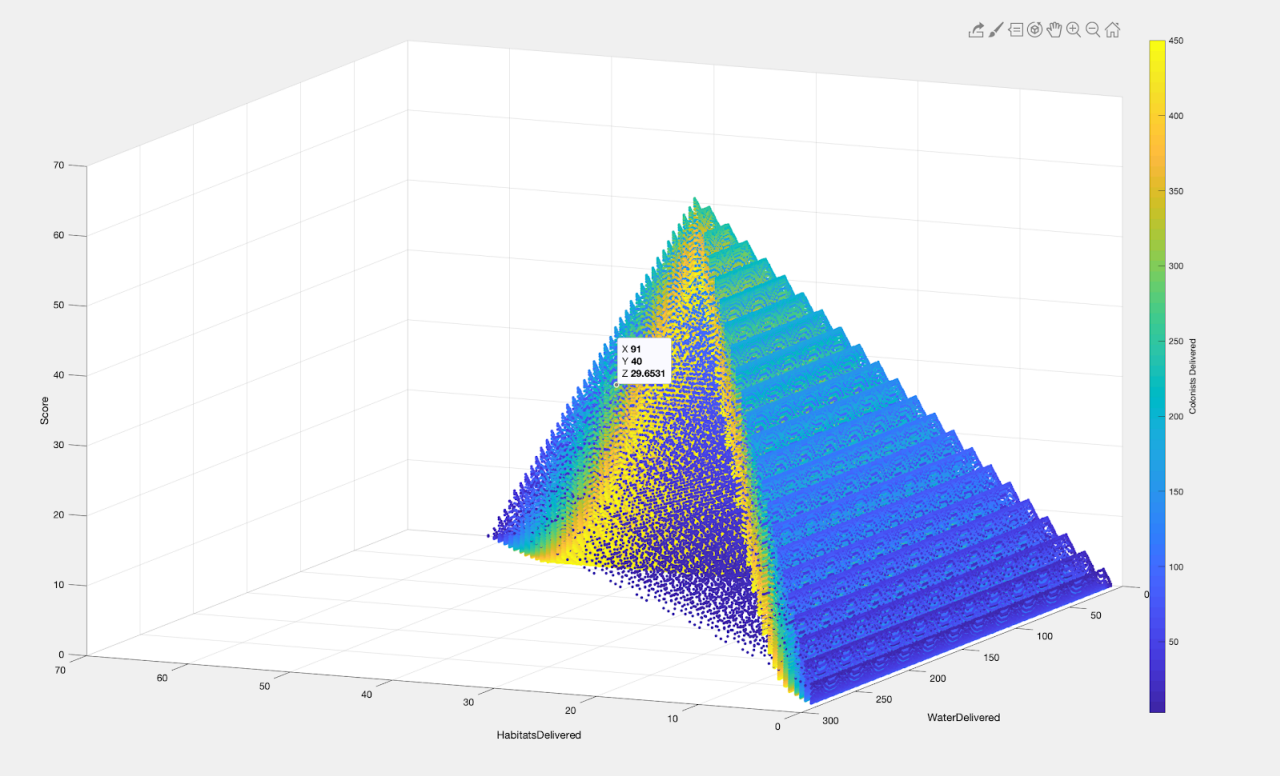

Figure 2: Plot of scoring function over the design space

The actual scoring will be tested by setting up a copy of the competition setup, and practicing dropping payloads (habitats and water) as well as colonist drones on the mock target area. The tests will be conducted under the same rules and regulations as the competition. Barring weather, radio interference, and the stress of being in-the-moment, the test setup should be nearly identical to the competition environment, yielding representative scoring results.

3.2.2 Design Sensitivity Analysis

Our scoring success strongly depends on our aircrafts wing planform area, fuselage carrying capacity, and the drop mechanisms. In addition, difficult flight scenarios including the craft's takeoff, turning, and landing characteristics can also lead to craft failure without scoring.

The wing planform must be able to carry the calculated payload and generate the lift to do so. When the craft is taking off or turning in air, depending on the thrust of the motor and the radius of the turn, the effective area producing the lift changes most in effectiveness, and it was looking at these cases that the wing planform was designed. The lift equation at an extreme of 30° produced the total area of the craft wing of 14.18 ft^2, the vertical area of that tilted wing being able to lift 25 lb payload. This adds a safety factor of 2, where based on the turning radius and speed, the craft needs to bank only 14.5° (equation **??**). The glider release mechanism being close to the fuselage is desirable, so airflow over the ailerons is not affected and the moment produced by these gliders about the center of the wing is minimized.

Fuselage volume and drop mechanism have historically been points of failure, needing careful attention. The payload at maximum theoretical carrying capacity comprises 18 habitats and 4 bottles containing 16.9 $floz$ water. These have an easily calculable volume and are arrayed in a compact tessellation, but the geometry of the fuselage must prevent the components from jamming while being released, and the mechanism must not be heavily influenced or impeded by the incoming airflow during flight.

3.3 Design Details

3.3.1 The Mothership

Each of the following subassemblies was designed by first conducting research to better understand their characteristics and discover alternate designs. We created decision matrices used to compare different configurations and weighted each in terms of factors such as simplicity, manufacturability and cost. We also performed experimental testing on the plane components -

wing, spar, and landing gear - to determine the amount of loads they could support. This topic is discussed further in section 4.1.

Wing

A decision matrix was used to select the airfoil shape. We used airfoiltools.com to find several airfoils that met our design criteria for maximum C_L/C_D, stall angle, and lowest C_D. From a set of ten airfoils, we were able to narrow our choice down to the Douglas LA203A Airfoil [3]. Table 3 shows the materials we considered for the wing and how they scored relative to criteria we set. We decided that EPS foam would be the best choice for our wing. To reduce the drag produced by the rough foam surface, we decided we would coat the wings with UltraCote.

Table 3: Wing Material Decision Matrix

Consideration	Weight	Low Density Foam and UltraCote		Balsa Ribs and Ultracote		Carbon Fiber Ribs and UltraCote		Carbon Fiber	
		Score	Weighted Score	Score	Weighted Score	Score	Weighted Score	Score	Weighted Score
Repairability	0.2	9	1.8	4	0.8	7	1.4	3	0.6
Time Required	0.7	10	7	4	2.8	7	4.9	6	4.2
Cost	0.1	10	1	9	0.9	6	0.6	3	0.3
Total	1		9.8		4.5		6.9		5.1

High Lift Device

We began our High-Lift Device (HLD) decision process by first researching different types of HLD mechanisms. After reading 'Aircraft Design' by Mohammad H. Sadraey [1] we were able to compile a decision matrix which allowed us to better evaluate each mechanism. The criteria used were: C_L increase, simplicity, and drag increase. As we expected, the highest scoring mechanism was the plain flap. The hinging mechanism used for these devices were plastic hinges epoxied to the foam, and UltraCote.

Tail

The decision process for the tail was driven by the desire for simplicity of design and fabrication, and lightweight. Due to the size of the propeller, the surface area of the vertical stabilizer and includes a 1.5 factor of safety on surface areas. Initially the team created a decision matrix

which proved that the optimal design was a conventional tail with rectangular vertical and horizontal stabilizers. After some testing, we realized that our vertical stabilizer was too small and that it required more surface area. We also strengthened the control surface (rudder) with a thin balsa sheet on each side.

Fuselage

Based on previous project's failures with carrying supply payload outside the fuselage, our team this year decided to design and build a bomb bay fuselage that was able to carry all the supply payloads we intend on dropping. This structure is made out of carbon fiber water jet ribs, covered with a thin layer of balsa wood epoxied into shape as shown in Figure 1.

Nose Cone

Similarly to our fuselage, our nose cone was also designed using a carbon fiber sheet rib structure. Some of this design's requirements are: needed to be strong and large enough to support and hold all the plane's electronics, needed to have easy access (to allow for in-between flights adjustments), and needed to be stable enough to hold the motor while on full throttle.

Fairing

This structure was also designed using a rib system, however instead of a balsa shell, it was covered using UltraCoat, since this structure will never have to support any load. It's addition to the design was made to improve the aerodynamics of the full plane design and also to increase the performance efficiency of the tail.

Landing Gear

The tricycle type landing gear was selected among the tail gear, quadricycle and multibougey type landing gears. Both nose and tail gears were obtained commercially and satisfy the necessary size and loading, requirements. Further empirical testing proved they are suitable for flight.

3.3.2 Colonist Drones

Designing the Colonist Delivery Drones required the balancing of strength, autopilot intelligence, and structural rigidity. The major decisions made were with respect to fuselage material and construction method, autopilot sensor suite, and lifting surface layout and size. The control surfaces were sized to carry the craft at a low angle of attack at flight speeds, since the lifting surfaces do not have airfoils. The fuselage needs to be stiff enough to hold shape during flight, and strong enough to survive landings without failure. This meant the material of the fuselage was very important, and since many of these crafts need to be built the method of manufacturing and assembly is also key. The amount of time to build and assemble the craft likely affects the craft's chance of success. The two major options considered were carbon fiber plates and tubes to build up a frame, and 3D printing PLA, Nylon, or Carbon fiber reinforced PEEK. The carbon fiber construction ensured stronger materials, but because of the density and the difficulty of implementing foam-core carbon fiber within our budget, carbon fiber structures ended up either overweight and over strengthened or not stiff enough to fly well. This paired with the complexity of assembling and manufacturing complex carbon fiber plate and tube structures made the implementation unfavorable when compared to 3D printing. Less dense plastics that are commonly 3D printed allowed for geometries that were stiff due to high bending moments of inertia, rather than simply favorable material characteristics. This allowed for both lightweight and stiff structures can be printed pre-assembled, requiring only the addition of electronics, lift surfaces, and a few carbon fiber reinforcing members. This allows for rapid iteration of design, and repeatability when assembling CDAs. Those characteristics, paired with a suitable weight of only 45 grams for the entire 3D printed fuselage made 3D printing the clear winner.

For electronics, a sensor suite needed to be paired with the chosen Pixracer autopilot. The pixracer running ardupilot was chosen because it is open source, allowing customization at any level, and because of it's good reputation with respect to features and reliability. While the au-

topilot choice was clear based on market availability and team member past experience, the sensor suite to pair with it was a much more nuanced decision. The two most important data streams the autopilot needs are an accurate location (e.g. lat. and long. coordinates) and an accurate altitude reading. Provided with those two data sets in real time, the autopilot should be able to navigate to the desired point given the craft has an adequate glide ratio to do so. The location choice of location sensor was clear as GPS is a standard, and there are few other widely used methods available in lightweight packages. To find altitude however there are many methods. The Pixracer itself has a barometer that can be used for altitude measurements, but due to barometric drift, the barometer altitude measurements can not be trusted to be accurate enough to facilitate precise landing maneuvers. This means another method must be researched. As the craft has a maximum weight of 9 oz., it is imperative the solution is both accurate and lightweight. This meant heavy sensor like microwave distance sensors were not a good fit. This left Lidar, ultrasonic, and other niche sensors left to be considered. LIDAR works well but cannot read over specular surfaces and is heavy, and since the competition sight is adjacent to water this was not a risk worth taking. Ultrasonic is light, works on all surfaces, and is accurate, but is not accurate at very low altitudes, where the precise reading is the most important. This left the last option, using RTK GNSS to calculate altitude. This allowed us to combine two sensors and save weight, while also recording data at the precision and accuracy needed to make delicate landing maneuvers.

3.3.3 Electronics

We do not have the funding to buy every motor we are interested in for testing. This left us relying on propeller data provided by manufacturers which only a few produced. Cobra and T-motor have the most detailed propeller data and we needed to make an initial decision based off these charts. The team chose the T-motor U8 Lite 190 KV this year. The motor provides significantly more thrust at a much higher efficiency and lower weight than other motors considered.

We paired it with a Castle Talon 60 amp ESC. A 40 amp ESC would have worked but we wanted the margin of safety. Seven Spektrum S6180 servos power control surface deflection. They were chosen because they provide high torque at an acceptable speed. Controlling the nose gear we chose a Savox SA-1230SG for it's excessively high torque and relatively high speed. Servo values in Table 4. We will be using two E-flite servoless payload release mechanisms for our glider release. The receiver controlling the propulsion loop is a Frsky X8R paired with a Taranis Q X7 transmitter. They were chosen because Frsky is open source and would allow for more configuration flexibility than other brands. We tested a straight line range of roughly 850 ft. Powering all this is a 6S 4,000 mah battery.

The telemetry loop consists of one lumenier LUX F7 flight controller, two RunCam Micro Eagle 800TVL, two Lumenier TX5GS video transmitters and one Matek M8Q-5883 GPS powered by a 3S battery. The GPS will report our altitude and distance to the target. Cameras with video transmitters will allow us to have an aerial view of the target. The flight controller allows GPS information to be displayed on the video feed.

Table 4: Servo Specifications

Servo	Torque	Speed
Spektrum S6180	100 oz-in	0.14s/60 degrees
Savor SA-1230SG	416.6 oz-in	0.20s/60 degrees

4 Assumptions and Design Restrictions

All analytical modeling and calculational dimensioning used a set of similar assumptions, including no head or tail winds, constant air conditions and properties, constant material properties within the craft, and standard temperature and pressure. Additionally, any flight modeling and sizing assumed a full battery, as is was sized to handle more than one flight for safety.

4.1 Load Bearing Capabilities

Based on the design of our wing and the maximum theoretical weight of the craft, a force of 13 lbf must accelerate a maximum of 25 lbf to takeoff speeds approximated to be 20.5 mph,

meaning that the fuselage must survive at least this force stretching it and include a safety factor. The wing must also survive loading at least equalling the weight of the rest of the craft, and though is allowed to deform a low amount to add a slight dihedral, must not deform more than 5° or fail in flight loads.

A hard landing, according to many airlines and the ICAO (International Civil Aviation Organization), has an acceleration of 2.6 g vertically down upon landing, and a severe landing as at least 2.86 g [6]. This sets a good guideline for the forces this craft, specifically its landing gear and frame, must be capable of withstanding upon landing. Assuming the theoretical maximum weight of 25 lbs under 1 g, a severe landing would a total of 71.5 lbs of load. With bought components comprising composite beams and hobbyist plane landing gear, the connections are the possible points of failure, and must be reinforced appropriately.

4.2 Environmental Impact and Considerations

The environmental impact of our aircraft depends on a number of factors ranging from materials used, amount of waste, and manufacturing methods. The plane is built mostly from in-organic materials such as carbon fiber, plastic (UltraCote), epoxy resin, and foam. This means that the recyclability of the plane is low, and materials will need to be disposed of with care, especially the resin infused materials that make up the bulk of the plane. These materials provide great mechanical properties, as well as favorable manufacturing qualities, meaning while they are not the best environmentally they are wonderful materials to work with when manufacturing lightweight and strong structures.

5 Analysis

5.1 Analysis Tools

5.1.1 Computational Methods

The modeling and simulation software used in designing the aircraft include SOLIDWORKS, Abaqus, and STAR CCM+. SOLIDWORKS was used to model the entire airplane and obtain the theoretical weight and moment of inertia of the aircraft. SOLIDWORKS was also used to perform stress analysis on our landing gear and carbon fiber spars, assuring that the parts will not fail under maximum loads. STAR CCM+ was used to analyze flow on our full plane cross-section, providing us with important estimates such as coefficient of lift and drag. Figure 3 image of a stress analysis simulation done on an assembly of the landing gear.

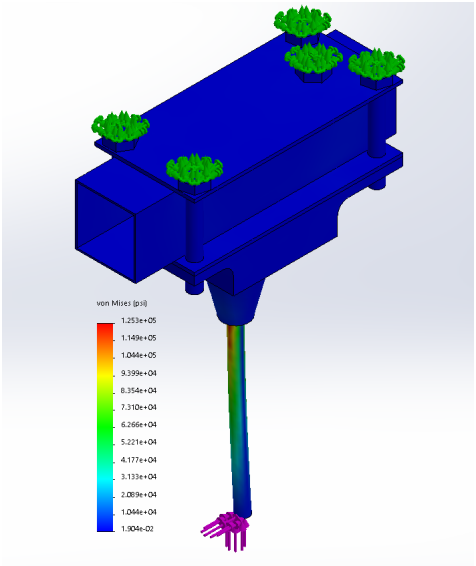

Figure 3: SOLIDWORKS simulation for the stresses acting on the landing gear

5.1.2 Developed Analytical Models

Modeling the craft provides baseline dimensioning and force specifications that testing or applying external research could not grant as quick or with as few resources. A team-written python model characterizing approximate takeoff behavior provided information on takeoff distance as a function of variable thrust curves, C_L and C_D vs. angle of attack curves, and craft vertical/horizontal surface areas.

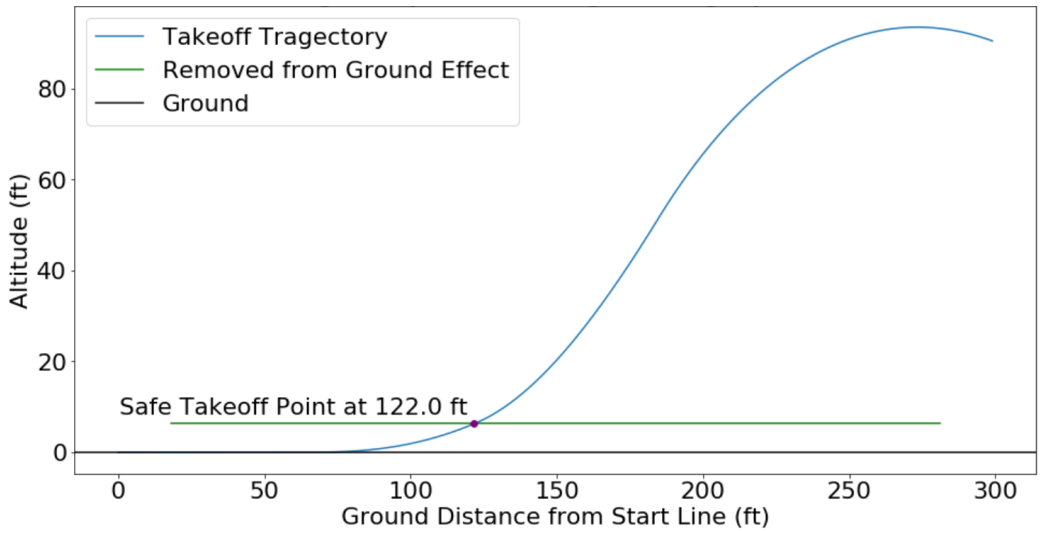

Figure 4: Using the Runga Kutta (four) Method, the vertical and horizontal equations of motion include lift, gravity, and a component of drag vertically, and thrust and drag horizontally, with a small component of lift based on angle of attack. This is limited to two dimensions, assuming a perfect symmetric craft and uniform conditions, without manipulating flaps except for elevator and HLD. This model has the throttle reduce after 50 ft high to level the craft, showing decaying oscillation to level flight after 500 ft.

The aileron dimensions were also computed with an analytical model in MATLAB that the team created, equating a banking moment acting on the craft to areas of its control surfaces showing $\frac{2}{3}$ maximum deflection. Control derivatives pertaining to a desired turning responsiveness produced the placement and construction of control surfaces in the wing and tail. the FAA(Federal Aviation Administration) provide baselines for response times for banking 30° or turning, equating to $\ddot{\theta}_{x,y,or\ z}$ used in the model. The moment of inertia of the craft was provided through SOLIDWORKS, completing the moment balance $\sum M = I\ddot{\theta}$. This assumes stable flight before the roll and turning, so surfaces evaluated deflecting at -20° to +25° have the ability to deflect more than -30° to +30°, and have areas 20% larger than calculated.

The ailerons were designed such that the pilot can achieve a bank angle of 15° in 1.3 seconds using a Matlab model based off textbook analysis methods [1], involving equation 9. This relates the forces of lift and drag to the moment of inertia and the roll rate of the aircraft. Solving for the dimensions of the ailerons involved an iterative process in which the length, chord and angle of maximum deflection of the ailerons changed while the dimensions of the wing, airspeed, air

properties and material properties remained constant. The bank angle was determined using equation 10 which relates flight speed (V) and expected turn radius (r) to the bank angle (θ).

5.2 Performance Analysis

During initial testing we used video to calculate takeoff and landing distances and speeds. Takeoff distance was approximately 45 ft with a speed of 30 ft/s, unloaded. Landing distance was 30 ft with a touchdown speed of 30 ft/s, unloaded. This matches predictions from analytical modeling in section 5.2.1 to within 5%.

5.2.1 Static and Dynamic Stability

The first part of the design process included the researching and decision making, but guaranteeing flight and scoring relies static and dynamic stability. Positive static stability drove integration of dihedral between the tail and wing, the wing's slight dihedral in flight, static margin, and vertical and horizontal tail surface areas. An initial static margin of -15% was a driver of dimensioning laterally from back to front, and lead to quality improvements to center the CG along the wing. The constructed craft boar a static margin of -8% because of changes of landing gear wheels and the drop mechanism, leading to a more controllable, less tail heavy plane, although slightly less stable. The dihedral along the wing in flight stems from our choice of material, the main box spar a carbon fiber square tube that 10.3 ft wings carrying 50 lbs (a safety factor of 2) deflects 2.25 inches, during stable flight creating a dihedral angle of 2.01 degrees. Dihedral between the wing and tail corresponds physically to a difference in incidence angles of 1.5° and the wing consistently having a larger lift coefficient for a given angle of attack. These stability-adding measures produced a craft that has a positive static stability, corresponding to interrupted stable flight causing the craft to initially be forced back to equilibrium. The goal was to equate the sum of all forces on the aircraft in stable flight to zero, slight changes in direction producing initial moments that correct back to equilibrium. These are modeled in python and tested briefly while hopping plain, with more tests scheduled.

Dynamic stability is more involved and resource intensive, though the desired combination of positive dynamic and static stability causes a craft to act as a dampened system, flight trajectory oscillations decaying based on correcting moments exerted on the craft. These were benefited by the previously mentioned design characteristics, and estimated using the control derivatives.

In addition, the static aeroelasticity of the craft was tested to ensure the maximum forces during flight would not significantly alter the designed specifications of the system. The durability of the 1 lb EPS foam was tested for deformation in the tail and wing under transverse loads, and individual wing segments were statically evaluated for plastic deformation. The Wing deformed up to three inches along its 11 foot frame under 75 lb transverse load, and it was applying mass to the tail that revealed the necessity for tension wires between the vertical and horizontal stabilizer, or else under flight conditions while, their relative deflection would be significant enough to reduce their control authority. The actual foam does not plastically deform except under point loads that would only be experienced under interaction with a foreign object like during a crash, and the flexure of the wing and tail do not permanently alter the foam construction. Dynamic aeroelasticity was tested on the ground restraining the craft from movement under full throttle, during common taxiing, and in the air during flight. Vibration on the ground was not recorded affecting structures except initially the nose cone, stabilizing after increasing throttle.

5.2.2 Lifting Performance and Margin

Using an induced drag coefficient at cruise speeds found with equation 3, the motor's dynamic thrust (equation 8) at full throttle would keep the craft at 30 mph as a maximum velocity. The plane carries a full weight of 25 lb at a minimum of 24 mph, but on an extreme bank angle of 30 degrees, we'd need 25.7 mph to maintain altitude. This is within 15 % of the theoretical maximum, but our calculated bank angle with a radius of 40 m is less than 15 degrees (equation

10). This confirms that the craft can carry its full designed payload, but with only a 15 % buffer before losing lift during a turn, it should not be the first load flown with in competition.

Analysis of maximum possible and acceptable speeds was done with a free body diagram equating the dynamic thrust to drag, solving for velocity, and checking how much the plane can lift at that speed. The acceleration the motor provides in takeoff changes with craft speed, and a takeoff analysis in section 5.1.2 uses dynamic thrust to model this behavior.

5.2.3 Motor Performance

When testing static thrust performance we tested a 26.4 x 9.4 in and a 28.4 x 10.1 in propeller. Data for the two propellers are located in figure 5. We decided to choose the 28.4 x 10.1 in propeller because it provides greater thrust using the same power. We also calculated the approximate top speed 30.2 mph. Since we are a small college we do not have access to certain equipment. The thrust stand owned by the team is inadequate and buying/building one was unfortunately not an option this year. Our work around was offsetting the thrust stand with a spring scale and the difference between maximum and minimum thrust gives the max static thrust. We also saw some arbitrary data before 500 W and we believe this is caused by the thrust stand shaking due to resonant frequency. The college also lacks a large wind tunnel capable of housing propellers of this size, so we have no experimental dynamic thrust data. We were, however able to find the take off speed provided by the motor and propeller through testing with the aircraft. Our take-off speed is 30 feet per second achieved in 4 seconds.

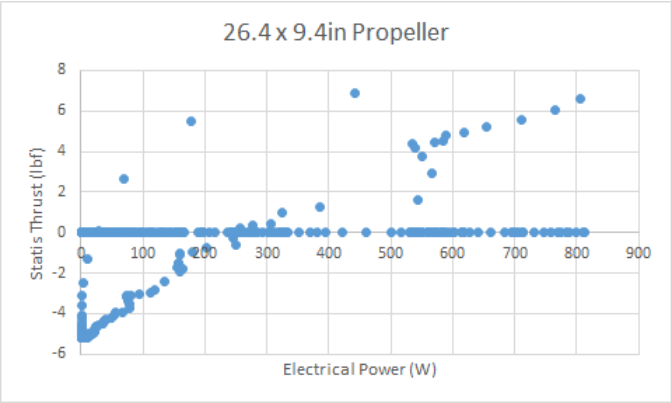

(a) Static Prop Data with Small Propellar

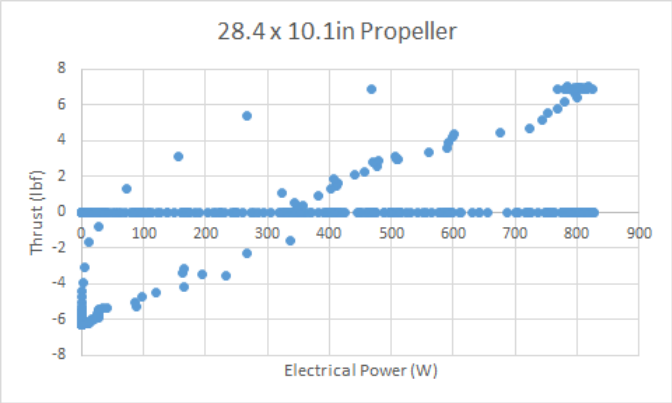

(b) Static Prop Data with Large Propellar

Figure 5: Prop Data

5.3 Assemblies Testing and Integration

The most important note we took from our Advanced team last year, was accessibility and assembly complexity. One of our primary goals when it came to assembly this year was to, create a design which required very little assembly complexity. Our team was able to accomplish this by designing sliding attachments instead of screwed or epoxied ones. Starting with the tail, this structure is made out of foam, as explained above, but it included small holes along the inside to allow for two carbon fiber rods to slide through and attach it to the bracket that would then connect both the horizontal and the vertical stabilizers to the tail boom.

The connection between the wing spar and the tail boom came with its challenges due to the existence of ribs at various distances inside the fuselage. Our team decided to manufacture two brackets out of aluminum that would slide through the wing spar and would then be bolted underneath the tail boom. Please note that the brackets include a number of cuts along its bottom surface to allow for the carbon fiber, fuselage ribs to slide onto it and help secure the full wing.

As mentioned previously, the fairing and the fuselage simply slide onto the tail boom and are sequentially secured in place by the nose cone. This structure not only slides onto the tail boom, but to provide the strength to secure the motor, it was also bolted to the tail boom.

6 Manufacturing

6.1 Structures

Nose Cone, Fuselage and Fairing

Ribs for the nose cone, fuselage and fairing were cut from 1/16th inch sheets of carbon fiber with foam cores using a CNC laser cutter. The skin on the nose cone and fuselage was made from layups of carbon fiber and epoxy using the vacuum bag method. To create space for the wing and landing gear, parts of the skin were cut using a rotary tool. Epoxy was used to secure longerons along the length of the fairing. Hot irons were used to adhere sheets of UltraCote onto the carbon fiber surface surfce and a heat gun was used to improve the surface tension and overall look.

Landing Gear

The team purchased landing gear designed to support the loads of similar aircraft. The tail gear bracket, which connects the tail gear to the boom, was cut and bent to shape using a 1/16 inch sheet of aluminum. The bracket connecting the nose gear to the carbon fiber boom was machined on a lath using aluminum. A bracket that holds the servo motor responsible to turn the nose gear was modeled on SOLIDWORKS and 3D printed using PLA.

Wing, Horizontal Stabilizer and Vertical Stabilizer

The wing, and tail surfaces were manufactured using EPS foam. Firstly, blocks of EPS were cut to suitable dimensions corresponding to the respective surface. Next, templates shaped to the airfoils we selected were cut from balsa wood using a CNC laser cutter. These templates were fixed to opposite ends of EPS blocks and sliced with hot nichrome wire resulting in complete sections of tail surfaces and multiple sections of the wing. Using the same method, the ailerons, elevators and the rudder were sectioned off. Afterwards, small sections of foam were cut for placement of the control horns and servo motors. The bracket that connects the wings to the fuselage was machined from a 1/16 inch sheet of aluminum. The tail bracket that connects the

horizontal stabilizer and the vertical stabilizer to the carbon fiber boom was 3D printed using PLA. A section of 1/16 inch sheet of carbon fiber with a foam core was laser cut and placed on the sides of this bracket for extra support.

6.2 Attachment Methods

Generally, our attachments were selected with the goal that the aircraft could be assembled and disassembled with ease. The nose cone, fuselage, and fairing meet and connect on the main tail boom. The ribs that make up the nose cone, fuselage and fairing were friction fit onto the carbon fiber boom. The skin that surrounds the nose cone and the fuselage was attached using epoxy. UltraCote is a thin sheet of plastic that contains an adhesive material found on one side which is activated by adding heat. This adhesive kept the UltraCote over the fairing. The wing was attached to the top surface of the fuselage and was held in place using a bracket that is fixed onto the boom using nylon bolts. In flight, these bolts will experience a shear stress of 50 lb but are rated to withstand 125 lb. The tail bracket was attached to the boom using epoxy. The vertical stabilizer and the horizontal stabilizer contain a set of carbon fiber rods which run through the length of these surfaces, and attach to the tail bracket, these rods are fixed in position using epoxy. The control surfaces were mounted into place using the Jacob's ladder method of attachment and by adding a hinge for support. Servo motors and control horns were mounted using epoxy. Finally, each surface was covered with UltraCote.

6.3 Glider

The CDA was designed with manufacturing in mind. The bulk of the glider is 3D printed, meaning it does not need to be assembled. The entire main fuselage as well as the mounting hardware for the electronics, and drop-connection hardware are all 3D printed and are slotted together using standard nylon nuts, bolts, and standoffs. This means the drones can be easily and reliably assembled. The remaining components are foam board cut for the aerodynamic

surfaces, standard diameter carbon fiber rods cut to length, and an UltraCote coating to seal in the colonists. This means the only non-trivial manufacturing or assembly step is covering the fuselage with UltraCote to seal and protect the colonists. As a result the colonist drones are remarkably easy to manufacture and assemble, which is important as up to six to eight of them need to be manufactured to have sufficient backups in case of unforeseen flight incidents.

6.4 Electronics

The electronics suite is assembled from off-the-shelf components. These components are all cross compatible, and only need to be soldered in the correct configuration before they can be used in flight. This type of system is favorable for a number of reasons. Firstly, the components are well known and trusted to be reliable in a myriad of situations. Secondly, the parts are modular and can be easily replaced by other market offerings. These parts are popular and much documentation and troubleshooting materials exist online to help when issues do inevitably occur. Those key benefits are why we chose to utilize a primarily off-the-shelf set of components.

7 Conclusion

In conclusion, we designed an aircraft capable of flight with total weight of 25 lbs, including 10 lbs of payload. The aircraft design was based on competition rules and criteria derived from the scoring algorithm mentioned earlier. Those constraints guided the design process, with the goal of having an aircraft that could score the maximum number of points. This required consideration of structural loads, dynamic stability, aerodynamics, telemetry and autonomous flight. By utilizing fundamental engineering principals with respect to solid and fluid mechanics, as well as open source autopilot systems and off the shelf components, a final design was realized that will be able to score well, with a predicted score of 59.4 points. This design has been validated by computational analysis, with experimental testing planned for the near future. Overall the robust design will be able to score reliably and favorably at competition because of the solid fundamentals on which it was designed.

Appendix A Table of Acronyms

STEM = Science, Technology, Engineering, and Mathematics
RC = Remote Controlled
UAV = Unmanned Aerial Vehicle
mph = Miles per hour
SAE = Society of Automotive Engineers
FOM = Figure of Merit
mAh = Milliamp-hour
LiPo = Lithium Polymer
ABS = Acrylonitrile Butadiene Styrene
ESC = Electronic Speed Controller
BEC = Battery Elimination Circuit
GPS = Global Positioning System
kV = Rotations per minute per volt
l or l_{opt} = Tail moment arm
K_C = Correction factor
$\overline{C}$ = Mean aerodynamic chord
S = Area of the wing
$\overline{V}_H$ = Horizontal tail coefficient
D_f = Maximum fuselage diameter
S_{HT} = Horizontal tail area
S_{VT} = Vertical tail area
C_{HT} = Horizontal tail coefficient
C_{VT} = Vertical tail coefficient
HLD = High Lift Device
C_w = Wing chord length
S_w = Wing area
b_w = Wingspan
CFD = Computational Fluid Dynamics
FEA = Finite Element Analysis
L = Lift force
PVC = Polyvinyl Chloride
CA = Cyanoacrylate
ASTM = American Society of Testing and Materials

Appendix B Equations

$$M_i = A_{wing} C_l \frac{\rho v^2}{2} 2 l_{COL} Sin(\theta) \tag{1}$$

Where A_{wing} is the top-view area of one of the wings, C_l is the coefficient of lift, ρ is air density which we assume equals about 1 kg/m^3, and l_{COL} is the orthogonal distance between the center of the fuselage and the wing's center of lift.

$$L = \frac{1}{2} C_L \rho V^2 A \tag{2}$$

$$D = \frac{1}{2} C_L A \frac{\rho V^2}{AR\ e_o} \tag{3}$$

$$e_o = \frac{1}{1.05 + 0.007 \pi A} \tag{4}$$

Where e_o is the Oswald Efficiency Factor and A is wing area.

$$l = l_{opt} = K_c \sqrt{\frac{4 \overline{C} S \overline{V}_H}{\pi D_f}} \tag{5}$$

K_c is the correction factor (chosen to be 1.4 as the after portion of the fuselage is non-conical), $\overline{C}$ is the mean aerodynamic chord of the wing (5.78 in), S is the area of the wing (225.8 in^2), $\overline{V}_H$ is the horizontal tail coefficient (1), and D_f is the maximum fuselage diameter (1.8 in).

$$S_{HT} = C_{HT} \frac{C_w S_w}{l} \tag{6}$$

$$S_{VT} = C_{VT} \frac{b_w S_w}{l} \tag{7}$$

For these equations, C_{HT} and C_{VT} are tail volume coefficients (chosen to be 1 and 0.08, respectively, based on coefficient values for transport planes), C_w is the wing chord length (5.171 in), S_w is the wing area (225.8 in^2), b_w is the wingspan (39 in), and l is the tail moment arm (30.08 in).

$$F_{thrust} = \rho * A_{prop\ circle} * \left(\frac{d}{3.29546 * pitch} \right)^{1.5} \left[(\omega * pitch)^2 - V_0 (\omega * pitch) \right] \tag{8}$$

Where ω is the prop rotations per second, $A_{prop\ circle} = \pi r_p rop^2$, and ρ is air density [5].

$$L_A + y_D \Delta D = I_{xx} \dot{P} \tag{9}$$

$$\theta = \arctan\left(\frac{V^2}{gr} \right) \tag{10}$$

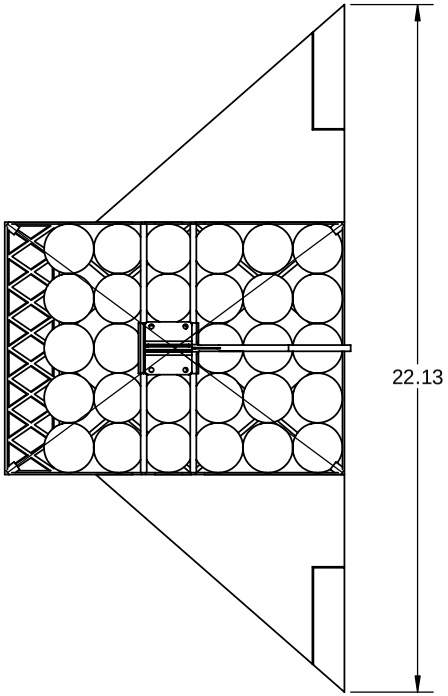

COMPONENTS
PIXRACER R15
RTK GNSS
1S LIPO
EMAX 9051 II

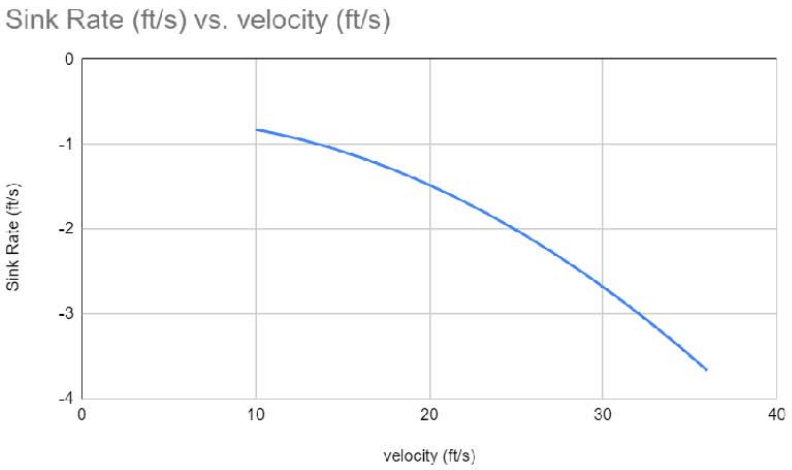

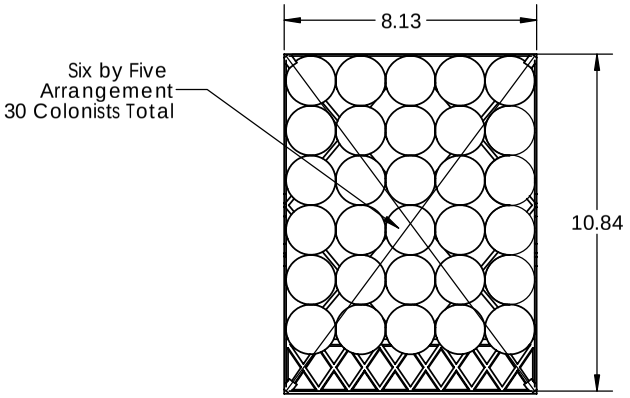

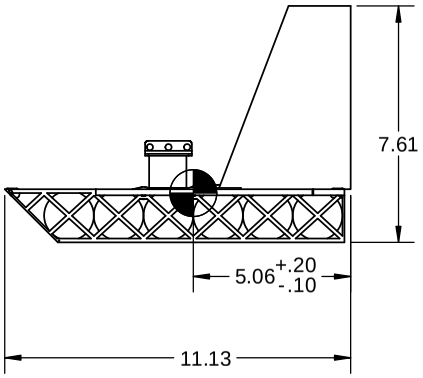

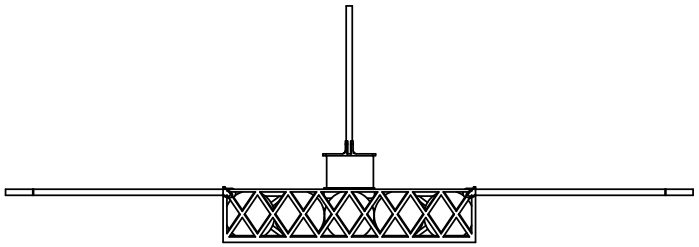

UNLESS OTHERWISE SPECIFIED DIM ARE IN INCHES		APPROVALS	DATE	UNION COLLEGE - DPT OF MECH ENGR			
.X	±.1	DRN BY: Mustafa Khan	2/19/20	TITLE: Glider Drawing			
.XX	±.01	CHD BY: Joana Santos	2/20/20				
.XXX	±.005	APPD BY:	XX/XX/XX				
.XXXX	±.0060	MATERIAL		SIZE B	TEAM NUMBER: 215		REV A
ANGULAR	±.3	FINISH		SCALE 1:4	WEIGHT 8.5 oz		SHEET 1 of 1
THIRD ANGLE PROJECTION		DO NOT SCALE DRAWING					

Stability Margin for Loaded CG and Empty CG
-8.3%

Weight and Balance Data Table			
Item	**Weight (oz)**	**Arm (in)**	**Moment (oz-in)**
Wing	65.6	.07	4.6
Tail	20.6	-70.0	-1442.0
Nose Cone	54.1	21	400.1
Fuselage	21.5	-4.0	-86.0
Fairing	4	-32.5	-130.0
Rear Landing Gear	22.9	-6.0	-137.4
Motor & Propeller	15.5	32.5	503.8
Battery & Electronics	31.8	28.5	906.3
Payload	160	0	0
Total	396.0		18.3

Summary Data Table	
Wingspan	123.92 in
Empty Weight	11.5 lbs
Battery Capacity	4000 mA-hr
Motor Make and Model	T-Motor U8 Lite
Motor KV	190KV
Propeller Manufacturer, Diameter, and Pitch	T-Motor, 28.4 inch diam., 10.1 inch pitch
Servo Information	Spektrum S6180, 100 oz-in

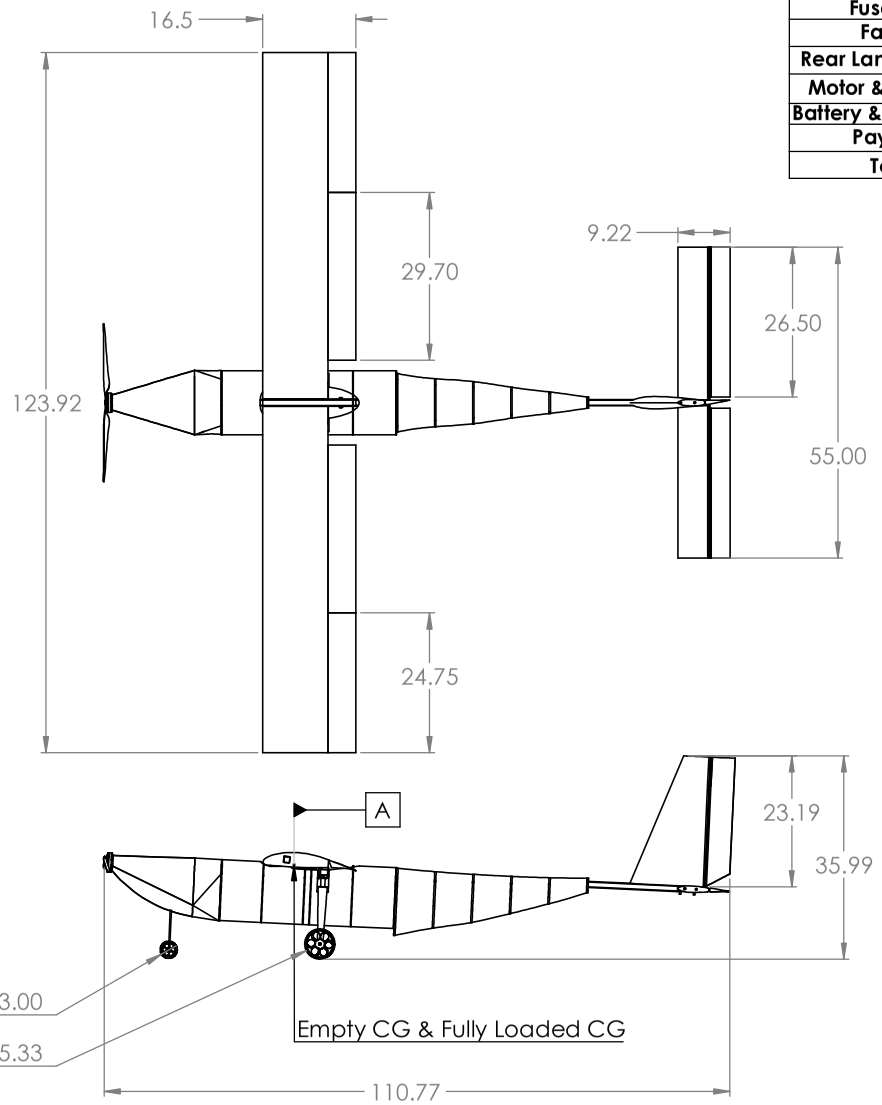

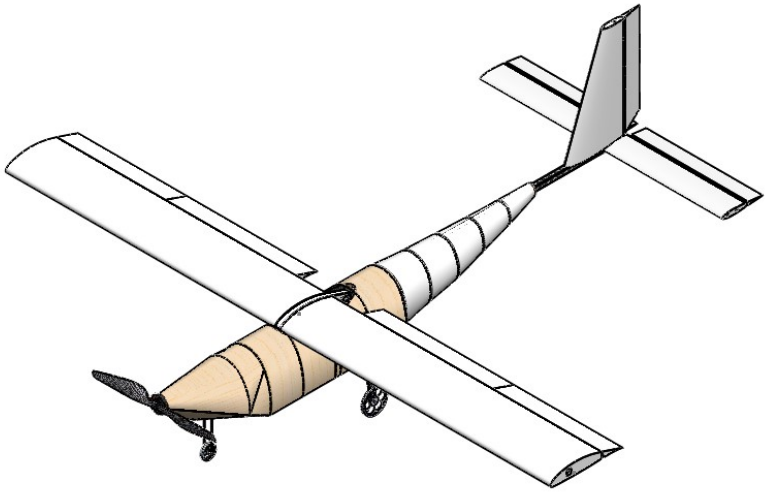

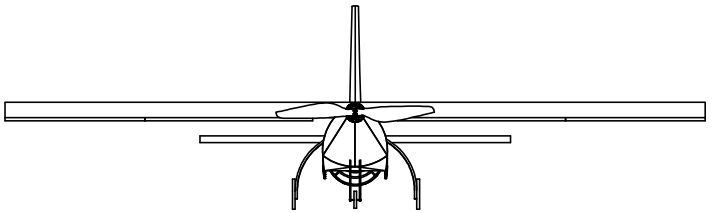

UNLESS OTHERWISE SPECIFIED DIM ARE IN INCHES	APPROVALS	DATE	UNION COLLEGE - DPT OF MECH ENGR
.X ±.1	DRN BY: Joana Santos	2/18/20	
.XX ±.03	CHD BY:	XX/XX/XX	TITLE: The Flying Dutchmen Advanced
.XXX ±.010	APPD BY:	XX/XX/XX	
ANGULAR ±.3	MATERIAL		SIZE B | TEAM NUMBER: 215 | REV A
THIRD ANGLE PROJECTION	COMMENTS		SCALE 1:22 | WEIGHT 15.5 lbs | SHEET 1 of 1
	DO NOT SCALE DRAWING		

Appendix C List of References

[1] Sadraey, M. H. *Aircraft Design: A Systems Engineering Approach* 1st ed. New York, NY: John Wiley & Sons Inc, 2012.

[2] Andersen, David. *Dihedral; Why, How Much, and Where?* RC Scale Builder.

[3] Airfoil Tools. "la203-il Airfoil" airfoiltools.com [Online] Accessed January 12, 2020. http://airfoiltools.com/airfoil/details?airfoil=la203a-il

[4] Nita, M. *Estimating the Oswald Efficiency Factor from Basic Aircraft Geometric Patterns* Hamburg University of Applied Sciences, The German Society for Astronautics and Aeronautics, 2012.

[5] G. Staples, *Propeller Static Dynamic Thrust Calculation*, July 2013. Accessed on: Nov. 24, 2019. [Online]. Available: https://www.electricrcaircraftguy.com/2013/09/propeller-static-dynamic-thrust-equation.html

[6] *"Flight Data Exchange (FDX)."* Saftey Reports, ICAO, May 2016, www.icao.int/MID/Documents/2016/RASG-MID5/RSA 06 - Flight Data Exchange (FDX).pdfsearch=hard landing definition.